Observer-Based Digital Ride-Height Control of a Fully Submerged Hydrofoil Boat

Shengwei Li and Hengfei Xu
School of Electrical and Computer Engineering
The University of Sydney, NSW, Australia

***Abstract*—Fully submerged hydrofoils give a small boat low drag and a smooth ride, but their lift hardly depends on depth, so the boat cannot hold a ride height without feedback. We model the heave and pitch dynamics of a solar-powered hydrofoil boat from first principles, with parameters of the Técnico Solar Boat SR02, including the loss of lift near the free surface, actuator limits, sensor noise and irregular head seas. Linearised at cruise speed, the plant is unstable and has four states but only three sensors, and the height sensor sees the water surface as well as the boat. We design a digital controller running at 50 Hz that combines linear quadratic state feedback with integral action and a Kalman filter with a force-bias state, and compare the filter with pole-placement observers. On the nonlinear model the controller settles a 5 cm height step in 2.2 s without overshoot, holds the height within 1 cm rms in regular waves and removes the steady-state error caused by speed and mass errors. Run as a separate real-time process connected to the simulated boat over a network link, the same controller reproduces these results exactly and tolerates replies one sample late.**

***Index Terms*—hydrofoil, ride-height control, LQR, Kalman filter, digital control, software in the loop**

I. Introduction

A hydrofoil lifts the hull out of the water and cuts its drag at speed, which matters most for boats with little power, such as the solar boats of student competitions [1], [2]. Surface-piercing foils regulate their own depth because their wetted span changes with height. Fully submerged foils are disturbed less by waves, but their lift is almost independent of depth [3]; a boat carried by them has almost no ride-height stiffness and must be stabilised by changing the foil incidence [1], [3].

Belime [1] modelled the SR02 boat of the Técnico Solar Boat team, designed an LQR with integral action at 7 m/s and flew it. In the trials the boat accelerated after take-off and left the speed the controller was designed for, so a separate speed loop on the motors was added; gain scheduling and an actuated rear foil were left as future work. Van Marrewijk and Schonebaum [2] derived and experimentally validated a dynamic model of a single-track hydrofoil boat. For larger craft, Ren and Yang [4] replaced a single LQR by fuzzy gain scheduling over the operating range of a hydrofoil catamaran, and Liu et al. [5] combined LQR output regulation with sliding-mode control to reduce the heave and pitch of a fully submerged hydrofoil craft in waves.

The single-point design of [1] is simple and has flown, but it is sensitive to speed. Gain scheduling [4] covers the speed range at the cost of a fuzzy model and an LMI stability test, and the sliding-mode design of [5] adds robustness, with weights tuned by a genetic algorithm, and was evaluated in simulation. On a small boat a further difficulty is the measurement: the ride height comes from a single ultrasonic sensor at the bow, which measures the distance to the water surface, not the height of the boat above its mean level. This paper treats that problem explicitly within the observer-based state feedback framework. Its contributions are:

1) a first-principles nonlinear heave and pitch model with free-surface effect and wave disturbances, checked against the trim of [1];
2) an observer-based controller in which a Kalman filter with a force-bias state separates the boat motion from the water surface, compared with pole-placement observers;
3) a direct digital design at 50 Hz with a computation delay, tested on the nonlinear model in regular and irregular seas and under model error;
4) a software-in-the-loop test in which the controller runs as a separate real-time process, which measures how late its commands may be.

Section II develops the model, Section III defines the control problem and the design criteria, Section IV designs the controller and observer, Section V validates them in simulation, and Section VI concludes.

II. System Model

A. Boat and assumptions

SR02 is a single-seat solar boat of 215 kg with pilot [1]. Two front foils, moved together, and one rear foil on the propulsion strut carry it when foil-borne (Fig. 1). The control inputs are the incidence angles δ_f, δ_r of the front and rear foils relative to the hull. We assume: (A1) the hull is clear of the water; (A2) the motion is in the vertical plane (heave and pitch); (A3) the forward speed U is constant, being held by a separate speed loop [1]; deviations are treated as model uncertainty; (A4) foil drag and thrust are neglected in the heave and pitch equations (their net moment is about 1 % of the foil moments); (A5) lift is quasi-steady and affine in the angle of attack below stall (12°); (A6) the added mass of the foils is neglected (4 % of the mass); (A7) the rear foil is actuated, which [1] lists as future work.

B. Equations of motion

The state is $\boldsymbol{x} = [\,h \quad v \quad \theta \quad q\,]^{\mathsf{T}}$: heave of the CM (up positive), its rate, pitch (bow up positive) and pitch rate. Foil

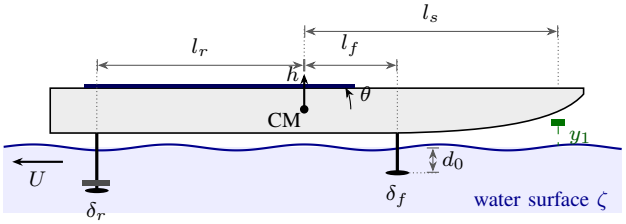


Fig. 1. Side view of the boat in body axes at trim: centre of mass (CM), front and rear foils, bow height sensor and the states h, θ.

$i \in \{f, r\}$ lies x_i ahead of and z_i below the CM. Its velocity relative to the water is

$$u_i = U + q\,(z_i \cos\theta - x_i \sin\theta), \quad v_i = v + q\,X_i - w_i, \quad (1)$$

where $X_i = x_i \cos\theta + z_i \sin\theta$ and w_i is the vertical water velocity from waves. The inflow angle $\gamma_i = \arctan(v_i/u_i)$ reduces the angle of attack, $\alpha_i = \delta_i + \theta - \gamma_i$, which damps heave and pitch. The lift is

$$L_i = \tfrac{1}{2}\rho\,(u_i^2 + v_i^2)\,S_i\,K(d_i/c)\,(C_{L0} + C_{L\alpha}\alpha_i), \quad (2)$$

with submergence $d_i = d_0 - h - x_i \sin\theta - z_i(1-\cos\theta)$ and the free-surface factor of linear foil theory at high Froude number ($U/\sqrt{g d_0} \approx 4.1$) [3],

$$K(\xi) = \frac{1 + 16\xi^2}{2 + 16\xi^2}, \qquad \xi = d/c, \quad (3)$$

which falls from 1 deep down to $\frac{1}{2}$ at the surface; in simulation $K = 0$ once a foil leaves the water. With $Z_i = x_i \sin\theta - z_i \cos\theta$, Newton's laws give

$$m\dot{v} = \textstyle\sum_i L_i \cos\gamma_i - mg, \quad (4)$$

$$I_y \dot{q} = \textstyle\sum_i L_i\,(X_i \cos\gamma_i + Z_i \sin\gamma_i), \quad (5)$$

with $\dot{h} = v$, $\dot{\theta} = q$. The nonlinearities are the trigonometric terms, the velocity-squared dynamic pressure, K, stall and the actuator limits.

C. Actuators, sensors and waves

The foil actuators have an absolute range of –3° to 7° [1]; we assume a rate limit of 20 °/s and, in simulation, a first-order servo lag of 20 ms. Encoders report the actual foil angles. The sensors, as fitted to SR02 [1], are an ultrasonic height sensor l_s ahead of the CM and an attitude reference unit (AHRS) giving pitch and pitch rate; we assume all are sampled at 50 Hz:

$$y_1 = h + l_s \sin\theta - \zeta(l_s, t) + n_1, \quad y_2 = \theta + n_2, \quad y_3 = q + n_3, \quad (6)$$

with white noise of standard deviation 1 cm, 0.3° and 0.2 °/s (assumed). The term ζ is the water surface under the sensor, which the height reading cannot distinguish from boat motion.

Waves are modelled by linear (Airy) theory in head seas as a sum of components,

$$\zeta(x,t) = \textstyle\sum_j a_j \cos(k_j x + \omega_{ej} t + \phi_j), \quad (7)$$

$$w_i(t) = -\textstyle\sum_j a_j \omega_j e^{-k_j d_0} \sin(k_j x_i + \omega_{ej} t + \phi_j), \quad (8)$$

TABLE I
MODEL PARAMETERS (B: FROM [1]; E: ESTIMATED OR ASSUMED)

m	215 kg	B	C_{L0}	0.288	B
I_y	503 kg m^2	B	$C_{L\alpha}$	5.16 rad^{-1}	B
S_f, S_r	0.096, 0.046 m^2	B	U_0	7 m/s	B
x_f, x_r	1.10, –2.45 m	B	c	0.073 m	E
z_f, z_r	0.75, 0.96 m	B	d_0	0.30 m	E
l_s	3.0 m	B	ρ	1025 kg/m^3	B

with $k_j = \omega_j^2/g$ and encounter frequency $\omega_{ej} = \omega_j + k_j U$. The regular test wave has 5 cm amplitude and 8 m wavelength ($\omega_e = 8.27$ rad/s, w amplitude 0.11 m/s). Irregular seas use 80 components of a JONSWAP spectrum ($\gamma = 3.3$) [6] with random phases.

D. Parameters, limitations and uncertainty

Table I lists the parameters. The chord follows from the lift slope and aspect-ratio correction of [1]; the submergence and the noise levels are assumed. The model is valid foil-borne, near level flight; it omits take-off, surge, unsteady lift, downwash of the front foils on the rear foil, ventilation and the horizontal orbital velocity (about 3 % of dynamic pressure in the test wave). The main uncertainties are the speed, which scales the control effectiveness with U^2, and the mass.

III. Problem Definition

A. Control aims and operating point

Without control the boat cannot hold a height (Section III-B). The height must stay inside a narrow window: a foil that comes too close to the surface loses lift and may ventilate, and a hull that drops by more than its clearance of about 0.3 m hits the water. The hull should also stay level, for the pilot and to keep both foils near their design angle of attack. The controller acts on δ_f, δ_r and measures y_1, y_2, y_3 and the encoders. It must reject waves, follow height commands from the pilot and cope with speed and mass changes.

The operating point is level flight at the endurance speed $U_0 = 7$ m/s [1] with the foils 0.30 m deep. Setting $\dot{v} = \dot{q} = 0$ in (4)–(5) shares the weight in inverse proportion to the lever arms, $L_{f0} = 1456$ N, $L_{r0} = 654$ N, and inverting (2) gives the trim incidences $\delta_{f0} = 3.53°$, $\delta_{r0} = 3.11°$. These agree with the numerical trim of [1], which includes drag and thrust, to within about 0.1° from 6 to 10 m/s (Table VI in the Appendix), supporting (A4). The front foil has only 3.5° of upward travel left at trim, and below 5.7 m/s level flight is impossible.

B. Linear model

With $\tilde{\boldsymbol{u}} = \boldsymbol{u} - \boldsymbol{u}_0$ and $\boldsymbol{w} = [w_f \;\; w_r]^\mathsf{T}$, linearising about trim gives $\dot{\boldsymbol{x}} = A\boldsymbol{x} + B\tilde{\boldsymbol{u}} + E\boldsymbol{w}$, $\boldsymbol{y} = C\boldsymbol{x} + \boldsymbol{n}$, with (angles in rad)

$$A = \begin{bmatrix} 0 & 1 & 0 & 0 \\ -0.239 & -12.17 & 85.21 & 2.893 \\ 0 & 0 & 0 & 1 \\ 0 & -0.228 & 1.321 & -14.47 \end{bmatrix}, \quad (9)$$

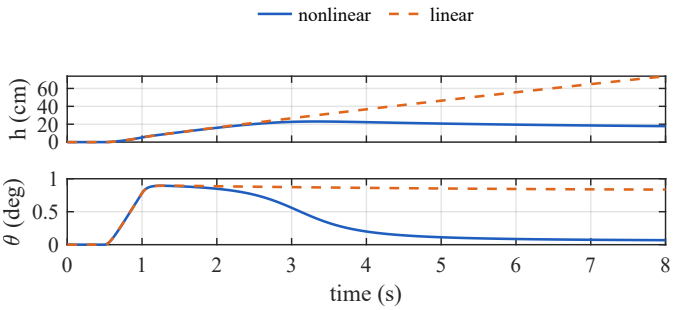


Fig. 2. Open loop: response to a 1° front-foil pulse of 0.5 s. The linear model drifts away; in the nonlinear model the foil nears the surface and loses lift.

$$B = \begin{bmatrix} 0 & 0 \\ 57.61 & 27.60 \\ 0 & 0 \\ 27.09 & -28.91 \end{bmatrix}, \; E = \begin{bmatrix} 0 & 0 \\ 8.230 & 3.944 \\ 0 & 0 \\ 4.180 & -3.952 \end{bmatrix}, \qquad (10)$$

$$C = \begin{bmatrix} 1 & 0 & l_s & 0 \\ 0 & 0 & 1 & 0 \\ 0 & 0 & 0 & 1 \end{bmatrix}, \quad l_s = 3\,\mathrm{m}. \qquad (11)$$

The matrices match a central-difference Jacobian of the nonlinear model to within 10^{-8}. The wave surface enters y_1 as a disturbance, $-\zeta$. Fig. 2 compares the two models: they agree until the heave exceeds about 15 cm, when the front foil nears the surface.

The eigenvalues of A are -14.81 and -11.80, the fast angle-of-attack responses, and -0.067 and $+0.027$. The slow pair is the ride height: the only restoring force is the free-surface term $\partial L/\partial d$, a stiffness of 51 N/m for both foils, so the height behaves almost as a double integrator and the plant is open-loop unstable. Whether the smaller slow pole is stable depends on the assumed c and d_0; the need for feedback does not.

C. Design criteria

From these aims we derive the criteria of Table II. R1 covers the expected speed and payload range. R2 lets the pilot change height in a few seconds; the overshoot bound keeps a 5 cm step within 5 mm. R3 is needed because a speed or mass error changes the lift needed at trim, which acts on the boat as a constant vertical force. R4 follows from the actuator limits. R5 bounds the height error so that three standard deviations (6 cm) stay within 20 % of the foil submergence and inside the range where the linear model holds.

IV. Controller Design

A. Reachability, observability and sensors

The reachability matrix $[B\ AB\ A^2B\ A^3B]$ has rank 4, also with either foil alone. The observability matrix of (A, C) has rank 4, also with any single sensor, so rank does not decide which sensors are needed. Robustness does. A speed or mass error acts as a constant vertical force b, which we add to the observer as a fifth state with $\dot{v} = \cdots + b$. With all three sensors the augmented pair (A_e, C_e) is observable (rank 5). With only the height sensor and the gyro it is observable but weakly: the slowest observer pole drops to about −0.005 rad/s, and in simulation a speed 1 m/s too low left the boat 12.6 cm low and pitched 2.4° while the estimates read zero. A force and a pitch offset produce the same bow reading; the AHRS pitch angle separates them. We therefore use all three sensors; heave and heave rate remain unmeasured ($n_y = 3 < n_x = 4$).

TABLE II
Design criteria (nonlinear model, actuator limits, sensor noise)

R1	Closed loop stable for $U \in [6, 9]$ m/s, $m \in [190, 240]$ kg.
R2	5 cm height step: 2 % settling within 2.5 s, overshoot below 10 %.
R3	Zero steady-state error in h and θ under speed and mass errors.
R4	Foil deflection within the 3.5° upward margin and rate within 20 °/s in normal operation.
R5	Height error below 2 cm rms in the 5 cm regular wave and in the mildest irregular sea (S1).

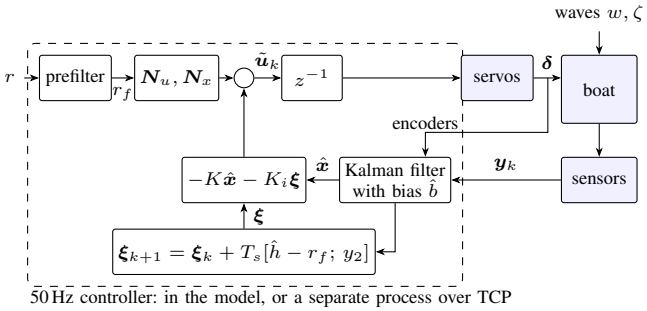


Fig. 3. Control loop. The dashed box runs every 20 ms; its command is applied one sample later. It runs inside the simulation or, in the software-in-the-loop test, as a separate process.

B. State feedback with integral action

The control law (Fig. 3) is

$$\tilde{\boldsymbol{u}} = \boldsymbol{N}_u r_f - K(\hat{\boldsymbol{x}} - \boldsymbol{N}_x r_f) - K_i\boldsymbol{\xi}, \quad \dot{\boldsymbol{\xi}} = \begin{bmatrix} \hat{h} - r_f \\ y_2 \end{bmatrix}, \qquad (12)$$

where r_f is the height command after a first-order prefilter ($t_f = 0.6$ s) and $\boldsymbol{N}_x, \boldsymbol{N}_u$ give the steady state for a height r with level pitch. The integrators act on the *estimated* height and the *measured* pitch: integrating the raw bow reading would make the boat follow the water surface. They are frozen while a command saturates (anti-windup). K and K_i minimise $J = \int (\boldsymbol{x}_a^{\mathsf{T}} Q \boldsymbol{x}_a + \tilde{\boldsymbol{u}}^{\mathsf{T}} R \tilde{\boldsymbol{u}})\, dt$ for the augmented model $\boldsymbol{x}_a = [\boldsymbol{x}; \boldsymbol{\xi}]$, which is reachable (rank 6). The weights follow Bryson's rule [7]: 2 cm of heave, 0.5 m/s of heave rate, 2° of pitch, 10 °/s of pitch rate and 3° of each foil. The integral weights, $10/0.02^2$ and $10/(1°)^2$, were tuned. The closed-loop poles are -3.32, $-3.90 \pm 2.35j$, $-10.8 \pm 5.6j$ and -18.5. The gains are physical: a height error moves both foils the same way, a pitch error moves them in opposite directions.

TABLE III

OBSERVER COMPARISON (NONLINEAR MODEL, 50 HZ). WAVES: 5 CM STEP IN THE REGULAR WAVE WITH NOISE. S2: IRREGULAR SEA, THREE SEEDS. SPEED ERROR: TRUE SPEED 6 M/S, PEAK HEIGHT DEVIATION AND TIME TO RETURN WITHIN 5 MM; WITH PP-KF THE HULL TOUCHED THE WATER AFTER 4.3 S.

	regular wave			S2	speed error
Observer	h err (cm rms)	$\hat{h}$ err (cm rms)	rate (°/s)	h err (cm rms)	peak / return
Kalman	0.99	0.71	4.6	2.0–2.3	15 cm / 7.6 s
PP-3x	4.28	3.35	19.2	8.9–9.5	2.8 cm / 0.7 s
PP-1x	3.41	3.67	19.3	8.6–10.2	4.1 cm / 1.2 s
PP-KF	2.71	0.72	18.3	2.1–2.2	diverges

C. Kalman filter with a force bias

The observer is a steady-state Kalman filter for the augmented model. The process noise is the wave velocity entering through E (variance $0.11^2/2$, correlation time 0.1 s) and a random walk on b of intensity b_{rate}^2, $b_{\text{rate}} = 0.5\,\text{m}\,\text{s}^{-5/2}$. The decisive choice is the height noise. The wave surface in y_1 has a variance of $\zeta_a^2/2$ concentrated in a band of about $\Delta f = 0.25$ Hz around the encounter frequency, so its spectral density there is $\zeta_a^2/(4\Delta f)$, about 100 times what the same variance spread as white noise would give. Using this value makes the filter trust the model and the AHRS at wave frequencies. The resulting observer poles are -0.66, $-0.67 \pm 0.62j$, -12 and -287: fast for the measured pitch, slow for the heave and the bias. The observer is slower than the controller, against the usual rule of thumb; the separation principle still applies, and the loop of plant, observer and integrators has exactly the poles of the two designs (difference below 10^{-12}). b_{rate} sets a trade-off: a larger value recovers faster from a speed change but follows long waves more.

D. Pole placement or Kalman filter

The usual design rule places the observer poles two to five times faster than the controller's. Table III compares three such observers with the Kalman filter, all with the same digital controller (Section IV-E): PP-3x and PP-1x place the five poles at 3 and 1 times the five slowest controller poles, and PP-KF at the poles of the Kalman filter.

The fast observers limit the deviation after a speed error to a fifth and recover ten times sooner, but they reconstruct the heave mostly from the bow reading and so follow the water surface (Fig. 4a): the height error in waves is four times larger and the foils run at the 20 °/s rate limit most of the time, which violates R4 and R5. PP-KF shows why pole locations are not enough with three outputs: its poles equal the Kalman filter's, yet the different gain matrix, i.e. different eigenvectors and a different weighting of the sensors, makes the foils chatter in waves and lets a speed error drive the hull into the water. The Kalman filter sets the gain from the noise statistics and is the only one that meets R5 and keeps the foil rate well below its limit; its price is a slower recovery from model errors.

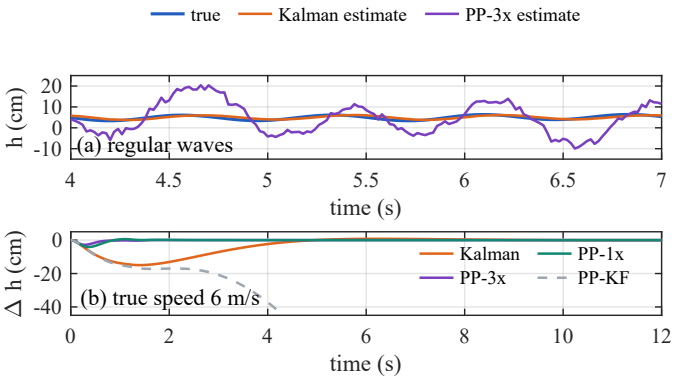


Fig. 4. (a) Heave estimate in the regular wave: the fast pole-placement observer follows the water surface. (b) Height deviation from the nominal response when the true speed is 6 m/s.

E. Digital implementation

The controller runs at 50 Hz. Running the continuous design with a 20 ms Euler step fails: the observer pole at −287 rad/s maps to $1 - 287 \cdot 0.02 = -4.74$, outside the unit circle (stability needs $T_s < 7$ ms). We therefore redesign in discrete time [8]. The plant is discretised with a zero-order hold; the LQR is computed with `dlqr` on the augmented model with weights QT_s, RT_s; the Kalman filter with `dlqe` in current-estimator form, with the process noise discretised exactly [9] and the measurement covariance R_n/T_s. The command computed from the samples at t_k is applied at t_{k+1}, and this delay is part of the design model through the extra state $\tilde{\boldsymbol{u}}_{k-1}$. Each sample the controller executes

$$\begin{aligned}\hat{\boldsymbol{x}}_{k|k-1} &= A_{de}\hat{\boldsymbol{x}}_{k-1} + B_{de}(\bar{\boldsymbol{\delta}}_k - \boldsymbol{u}_0),\\ \hat{\boldsymbol{x}}_k &= \hat{\boldsymbol{x}}_{k|k-1} + M(\boldsymbol{y}_k - C_e\hat{\boldsymbol{x}}_{k|k-1}),\\ \tilde{\boldsymbol{u}}_k &= \boldsymbol{N}_u r_f - K_d(\hat{\boldsymbol{x}}_k - \boldsymbol{N}_x r_f) - K_{id}\boldsymbol{\xi}_k\\ &\quad - K_u(\tilde{\boldsymbol{u}}_{k-1} - \boldsymbol{N}_u r_f),\end{aligned}$$

followed by the integrator and prefilter updates, where $\bar{\boldsymbol{\delta}}_k$ is the mean encoder reading over the last interval. The equivalent poles of the digital LQR match the continuous ones within 1 %. Those of the filter are $-0.67 \pm 0.62j$, -1.28, -12 and -178; the difference from the continuous filter is a sampling effect and vanishes as $T_s \to 0$.

Table VII in the Appendix repeats the design and the wave test at other rates. The error grows gradually down to 15 Hz. At 10 Hz the loop fails although the design model is stable: the servo lag, which the design model omits, then destabilises a mode at the Nyquist frequency (5 Hz, $|z| = 1.04$). We keep 50 Hz, three times above the slowest acceptable rate; 100 Hz would gain only 0.05 cm.

F. Stability margins

Breaking the digital loop at the input of one foil, the other loop closed, gives $L(z)$ with the servo lag, the Kalman filter, the integrators, the gains and the computation delay (Bode plot in Fig. 10, Appendix). The front-foil loop has two unstable open-loop poles and is stable by Nyquist's criterion (two

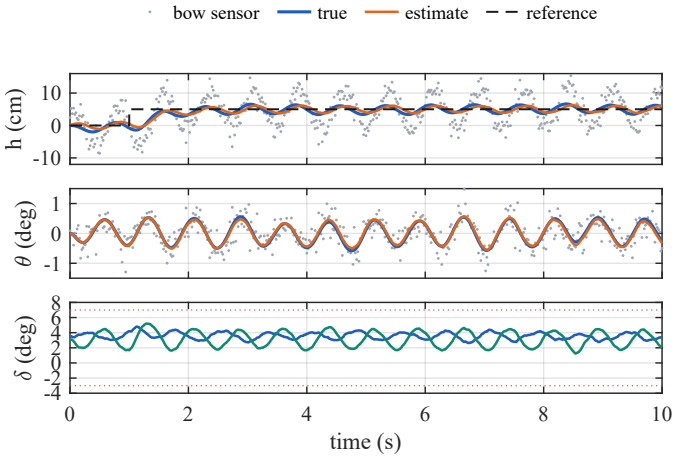


Fig. 5. 5 cm step in the regular wave with sensor noise: height from the bow sensor (dots), true and estimated height and pitch, and foil angles (blue: front, green: rear; dotted: position limits).

counter-clockwise encirclements of -1). Its gain margins are -15.2 dB at 0.35 Hz and 10.1 dB at 5.2 Hz, and its phase margin 39.5° at 1.9 Hz allows 2.9 samples of extra delay. The rear-foil loop has 15.6 dB and 68.9°. A common factor a on both commands keeps the loop stable for $0.05 < a < 3.2$; the input sensitivity peaks at 5.3 dB.

V. Numerical Validation

All tests use the nonlinear model (1)–(6), integrated with `ode45` between samples, with sampled noisy sensors, actuator limits, rate limit and servo lag. The same model built in Simulink agrees with the MATLAB simulation to 1×10^{-10} m in open loop and 0.33 mm in closed loop with waves. The MATLAB and Simulink files that accompany this paper reproduce every figure and table.

A. Tracking and regular waves

Fig. 5 shows a 5 cm step in the regular wave. In calm water the step settles in 2.16 s without overshoot (R2). In waves the height error is 0.99 cm rms and the pitch 0.33° rms (R5). The heave estimate ignores most of the ±10 cm scatter of the bow reading. The front foil moves by at most 1.3° from trim (R4); its rate is 4.6 °/s rms and reaches the 20 °/s limit only in short peaks.

B. Estimation error

To check that the estimation error converges, Fig. 6 starts the boat 5 cm high and 1° bow-up while the estimate starts at zero, in the regular wave with noise. The pitch error falls below 0.1° within 2 s and the heave error within about 1.5 s to a bounded oscillation at the encounter frequency, the part of the wave surface the filter cannot separate from boat motion. After 3 s the errors are 0.82 cm, 1.7 cm/s, 0.05° and 0.21 °/s rms for h, v, θ and q.

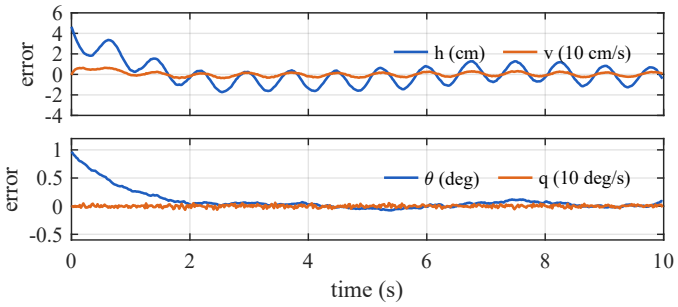


Fig. 6. Estimation errors from a wrong initial estimate (boat 5 cm high, 1° bow-up), regular wave with noise.

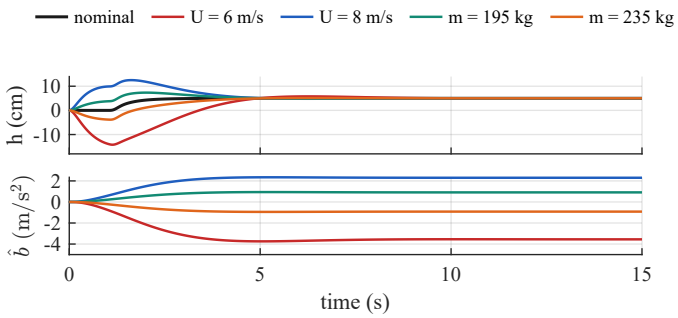


Fig. 7. 5 cm step with speed and mass errors (calm water) and the estimated force bias $\hat{b}$.

C. Model uncertainty

Fig. 7 repeats the calm-water step with the true speed or mass away from the design values. The bias estimate converges to the force each error causes and the integrators remove the remaining error: height and pitch return to their targets in every case (R3). The worst case, a speed 1 m/s too low, gives a 15 cm transient that is back within 5 mm after 7.6 s. This is the cost of the slow observer (Table III); scheduling the trim angles on the measured speed would remove most of it.

D. Irregular seas

Table IV gives the results in three JONSWAP sea states, five random seas each. In S1 the error matches the regular wave (R5). It then grows faster than the wave height, because the longer waves of S2 and S3 are met at lower frequencies, where the filter cannot tell the water surface from slow boat motion. Pitch, which is measured, stays below 0.4° rms. In S3 the front foil reaches its limit for up to 0.5 % of the time. Fig. 8 shows S2: the estimate follows the slow part of the boat motion but not the ±10 cm water surface, and the front foil uses at most about two thirds of its upward margin.

E. Software in the loop

To test the controller as it would run on the boat's computer, we moved it into a separate MATLAB process. The Simulink model of the boat sends the sensor and encoder readings every 20 ms over TCP and applies the reply at the next sample, which is the delay of the design; the controller never sees the true state. Two modes are used. In *lockstep* the model waits for each

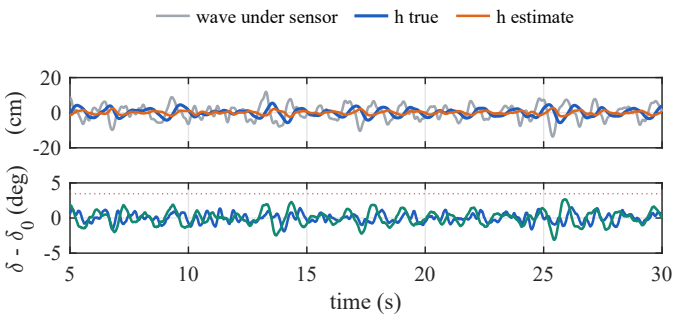


Fig. 8. Sea state S2 ($H_s = 0.15\,\mathrm{m}$, $T_p = 3\,\mathrm{s}$): water surface under the sensor, true and estimated heave, and foil deflections from trim (blue: front, green: rear; dotted: upward limit of the front foil).

TABLE IV
IRREGULAR HEAD SEAS: RANGE OVER FIVE SEAS (AFTER 5 S)

Sea	H_s (m)	T_p (s)	h err rms (cm)	θ rms (deg)	foil peak (deg)	sat. (%)
S1	0.10	2.3	0.72–0.81	0.20–0.21	1.5–2.3	0
S2	0.15	3.0	1.8–2.2	0.25–0.28	1.8–2.5	0
S3	0.25	3.5	3.6–4.9	0.34–0.40	2.6–4.7	0–0.5

reply; the trajectory is then identical to the in-model controller (difference exactly zero), which shows that the split changes nothing. In *real time* the model is paced to the wall clock and holds the last command when a reply is late. A round trip takes 0.24 ms (median) and the control algorithm 0.1 ms, and 99 % of the 20 ms steps keep to the clock within 0.6 ms.

We then slowed the controller down (Fig. 9). Up to 18 ms of computing time nothing changes. From 22 ms to 35 ms every reply is one sample late, yet the height error stays at 0.94–0.99 cm. At 40 ms it doubles (2.1 cm) and at 50 ms the boat oscillates by ±10 cm. A linear analysis with n extra samples of delay agrees: the damping ratio of a 2 Hz mode falls from 0.62 to 0.32, 0.11 and -0.03 for $n = 0$ to 3, as the delay margin of 2.9 samples predicts. Random computing times of 10 to 30 ms made 80 % of replies late, because a late reply delays the next one, with an error of 1.00 cm. The controller must therefore finish within one period, with one sample of tolerance; its actual time on the boat's microcontroller should be measured. Both processes ran on one computer, so network delays and clock drift of a real system are not represented. A 3D browser view of the run, which takes no part in the loop, is shown in Fig. 11 (Appendix; folder `viz`).

F. Limitations of the validation

All results come from simulation, so they are only as good as the model. Three assumptions deserve comment. First, lift is quasi-steady: at the encounter frequency of the test wave the reduced frequency is $\omega_e c/(2U) \approx 0.04$, low enough for unsteady lift to be small, but shorter waves or a faster boat would need an unsteady model. Second, the waves are linear, long-crested and from ahead, without roll; oblique seas would couple roll into the bow-height reading. Third, the chord, the submergence, the sensor noise and the actuator rate are

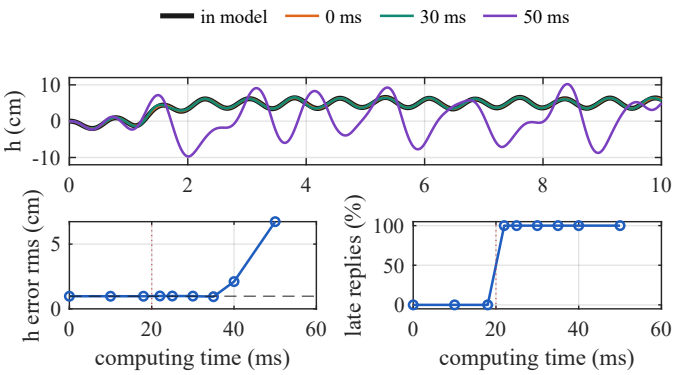


Fig. 9. Controller as a separate real-time process with added computing time: height for three cases, height error and share of late replies.

TABLE V
DESIGN CRITERIA AND RESULTS

	Result	Met
R1	largest pole magnitude 0.989 over the grid	yes
R2	settling 2.16 s, no overshoot	yes
R3	zero error for $U = 6,8\,\mathrm{m/s}$, $m = 195,235\,\mathrm{kg}$	yes
R4	deflection 1.3°; rate limit reached in short peaks	partly
R5	0.99 cm (regular), 0.72–0.81 cm (S1)	yes

estimates. The main design conclusion, that the observer must not follow the water surface, rests on the ratio between the wave surface and the boat motion in the height reading, which is set by the wave and not by these values; the numbers in Tables III and IV would change with them. The ultrasonic sensor is modelled as a point measurement with white noise, while a real sensor averages over its beam footprint and may drop out in spray. Testing on the boat is the necessary next step.

VI. CONCLUSIONS

A fully submerged hydrofoil boat is open-loop unstable in heave, and its only height sensor sees the waves. An LQR with integral action on the estimated height and measured pitch, combined with a Kalman filter that models the water surface as narrow-band noise and estimates a force bias, meets the design criteria on the nonlinear model at 50 Hz with a computation delay (Table V); the rate limit is touched only in short peaks. Pole-placement observers designed by the usual rule recover faster from model errors but follow the water surface and saturate the actuators, and placing the poles where the Kalman filter puts them is not enough. Run as a separate real-time process, the controller reproduces the in-model results and tolerates one sample of extra delay. Future work: scheduling the trim and gains on the measured speed, which would shorten the 8 s recovery from speed errors; a second height sensor or an accelerometer for long waves; and tests on the boat's microcontroller.

References

[1] B. J. Belime, "An hydrofoil control system for the SR02 vessel in the scope of the Técnico Solar Boat Project," M.Sc. thesis, Instituto Superior Técnico, Univ. Lisboa, Lisbon, Portugal, 2020.

[2] G. P. van Marrewijk and J. K. Schonebaum, "An experimentally validated dynamical model of a single-track hydrofoil boat," TU Delft Solar Boat Team, Delft Univ. Technol., Delft, The Netherlands, 2017.

[3] O. M. Faltinsen, *Hydrodynamics of High-Speed Marine Vehicles*. Cambridge, U.K.: Cambridge Univ. Press, 2005.

[4] J. Ren and Y. Yang, "Fuzzy gain scheduling attitude control for hydrofoil catamaran," in *Proc. Amer. Control Conf.*, Boston, MA, USA, 2004, pp. 1103–1108.

[5] H. Liu, Y. Fu, and B. Li, "Study of the LQRY-SMC control method for the longitudinal motion of fully submerged hydrofoil crafts," *J. Mar. Sci. Eng.*, vol. 10, no. 10, Art. no. 1390, 2022.

[6] K. Hasselmann *et al.*, "Measurements of wind-wave growth and swell decay during the Joint North Sea Wave Project (JONSWAP)," *Ergänzungsheft zur Deutschen Hydrographischen Zeitschrift, Reihe A*, no. 12, 1973.

[7] A. E. Bryson and Y.-C. Ho, *Applied Optimal Control*. Washington, DC, USA: Hemisphere, 1975.

[8] G. F. Franklin, J. D. Powell, and M. L. Workman, *Digital Control of Dynamic Systems*, 3rd ed. Menlo Park, CA, USA: Addison-Wesley, 1998.

[9] C. F. Van Loan, "Computing integrals involving the matrix exponential," *IEEE Trans. Autom. Control*, vol. 23, no. 3, pp. 395–404, Jun. 1978.

Appendix
Supporting Tables and Figures

TABLE VI
TRIM INCIDENCES (DEG): THIS MODEL AND [1]

U (m/s)	6	7	8	9	10
δ_{f0}, this model	5.97	3.53	1.96	0.87	0.10
δ_{f0}, [1]	5.9	3.5	1.9	0.8	0.1
δ_{r0}, this model	5.39	3.11	1.63	0.62	−0.11
δ_{r0}, [1]	5.5	3.2	1.7	0.7	0.0

TABLE VII
CONTROLLER RATE: 5 CM STEP IN THE REGULAR WAVE WITH NOISE, DESIGN REDONE FOR EACH RATE

Rate (Hz)	100	50	25	20	15	10
h error (cm rms)	0.94	0.99	1.09	1.17	1.34	16.8
θ (deg rms)	0.30	0.33	0.39	0.45	0.49	2.42

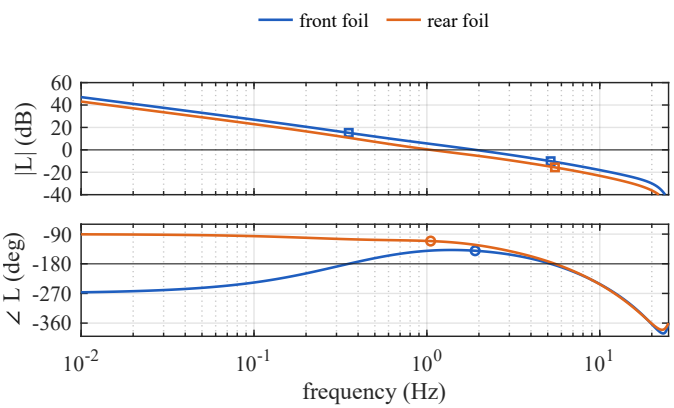


Fig. 10. Bode plot of the digital loop broken at the input of the front foil (blue) and of the rear foil (orange), the other loop closed. Squares: gain margins; circles: phase margins.

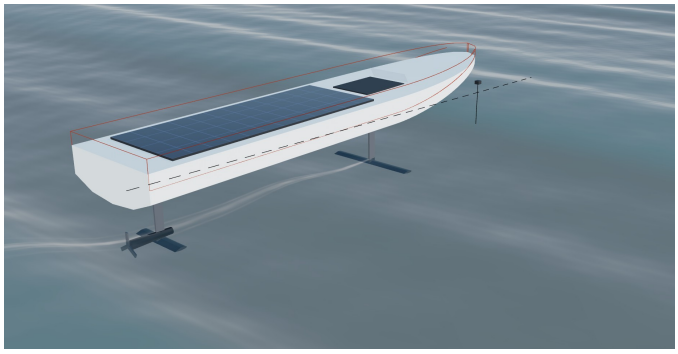


Fig. 11. 3D view of a software-in-the-loop run in sea state S2, heave and pitch drawn three times larger than simulated. White hull: true state; orange outline: the controller's estimate; vertical line at the bow: ultrasonic measurement; dashed line: target height. The large-scale water surface is the simulated wave field; the ripples and strut wakes are drawn for appearance only.